PERFORMANCE OF LOW-RISE BUILDINGS WITH NO SEISMIC DESIGN IN UNANTICIPATED EARTHQUAKES

C. C. Simsir[(1)], B. Arya[(2)], A. Jain[(3)]

[(1)] *Senior Consultant, Walker Consultants, csimsir@walkerconsultants.com*
[(2)] *Senior Consultant, Walker Consultants, barya@walkerconsultants.com*
[(3)] *Vice President, Walker Consultants, ajain@walkerconsultants.com*

Abstract

This paper presents the seismic performance of low-rise buildings in Oklahoma, United States during the M5.0 Cushing Earthquake of 6 November 2016. These one- to two-story buildings were typically designed and constructed in the last 65 years with little or no consideration for seismic actions because they are located in an intraplate region with limited seismic history until recently. In the last ten years, rates of earthquakes increased rapidly in Oklahoma due to increased petroleum exploration and extraction activity; consequently, the short-term seismic hazard maps for the region were updated in the last three years to account for earthquakes induced by this prospecting activity. The Cushing Earthquake was the fourth largest of these induced earthquakes and felt in a large region including Oklahoma, its neighboring states, and as far away as Indiana due to the geology of the Central and Eastern United States. The structural systems of the low-rise buildings under consideration varied, typically consisting of gravity load carrying steel columns or unreinforced masonry (URM) bearing walls which support steel beams, open-web joists, or precast concrete joists for roof framing. On-site observations showed that the earthquake caused structural and non-structural damage to these buildings located 3 to 6 kilometers away from the epicenter. The earthquake produced peak ground accelerations as large as 0.58g as recorded in the vicinity of the buildings and spectral accelerations over 2g in the frequency range of 7 Hz to 20 Hz. These dominant frequencies of the earthquake ground motion coincided with the natural frequencies of vibration of these buildings, all of which had URM walls either as load bearing, non-load bearing or veneer walls. This caused horizontally cracked and out-of-plumb masonry walls due to out-of-plane action and stair-stepped shear cracking of the walls due to in-plane action. The lighter-weight, flexible roof diaphragms resulted in amplified out-of-plane accelerations in masonry walls and racking of steel gravity columns, while the heavier precast concrete roof joists resulted in increased seismic mass and in-plane shear force demand in the walls. Out-of-plane damage was most prominent in the wall piers between window openings. Out-of-plumb shifting of brick veneer walls were also observed to have caused further damage to the concrete masonry bearing walls along their bedjoints where the veneer is attached with masonry ties. At some locations of roof framing bearing on masonry walls, observations revealed cracking of the masonry walls and spalling of the precast concrete roof joists. Damage to interior finishes was widespread with cracked drywalls, separations at seams of partition wall panels, racked and fallen ceiling panels, and separations of the roof framing and utility lines from the interior finishes. Nonlinear structural analyses of the masonry walls, represented as single-degree-of-freedom systems with strength and stiffness degradation characteristics, assisted in the assessment of damage and evaluation of repairs. This paper summarizes the lessons learnt and identifies the types of damage the buildings sustained, the seismic factors and structural vulnerabilities that contributed to damage, structural analysis to evaluate damage, and methodologies for repair and strengthening considering the increased current earthquake hazard for the region.

Keywords: Low-rise buildings; Unreinforced masonry; Induced earthquake; Damage assessment

1. Introduction

This paper presents the findings from a damage assessment of a dozen low-rise buildings in Oklahoma, United States, historically a region of low seismic risk, which was affected by the M5.0 Cushing Earthquake of 6 November 2016.

The United States Geological Survey (USGS) reported one injury, at least 40 severely damaged buildings, and power outages occurring in the City of Cushing during the earthquake [1]. Some of the buildings in the Central Business District (CBD) of Cushing were demolished following the earthquake due to the heavy damage and partial collapse that they sustained. These buildings were typically of a century old unreinforced masonry (URM) brick construction with wood-framed floor and roof diaphragms. The focus of this paper is on other, relatively newer (circa 1955 to 1990) low-rise buildings having unreinforced or partially reinforced masonry walls as their main lateral force resisting systems that were investigated by the authors.

This paper summarizes the lessons learnt and identifies the types of damage the buildings sustained, the seismic factors and structural vulnerabilities that contributed to damage, structural analyses to evaluate damage, and methodologies for repair and strengthening considering the increased current earthquake hazard for the region.

2. Earthquake Data

The moment magnitude 5.0 Cushing Earthquake occurred at 7:44 pm on 6 November 2016. The earthquake hypocenter was at a shallow depth of 4 km and the epicenter was located only 3 km from the Central Business District (CBD) of Cushing in Oklahoma. The earthquake occurred as a result of shallow strike-slip faulting within the interior of the North American continental plate, far from any plate boundaries as reported by USGS [1]. In the last 10 years, the rates of earthquakes increased rapidly in Oklahoma, majority of which have been linked to increased petroleum prospecting activity. The increased level of seismicity and the associated damage to building stock from some of these earthquakes in Oklahoma was illustrated in literature [1, 2]. The Cushing Earthquake was the fourth largest of these recent induced earthquakes and felt in a large region including Oklahoma, its neighboring states, and as far away as Indiana due to the intraplate geology of the Central and Eastern United States.

Fig.1 presents the horizontal peak ground acceleration (PGA) contour map developed by USGS for this seismic event [1]. Fig.1 also shows the location of Cushing CBD with respect to the Cushing Earthquake epicenter. Based on the data recorded at the three seismic stations which are closest to Cushing, the horizontal PGAs were 0.58g, 0.46g, and 044g. All three stations and almost the entire City of Cushing are located within the innermost contour of 0.42g in the PGA map in Fig.1. Recorded ground acceleration histories in the East-West and North-South directions are presented in Fig.2 for station OK914 which recorded the largest PGA [3]. The largest vertical PGA recorded was 0.31g [3].

The USGS reported the ground shaking intensity at a Modified Mercalli Intensity (MMI) of VII (7) for this earthquake event based on the shaking perceived by the people in the area and the expected Moderate Damage to structures [1]. The PGAs in the range of 0.42g to 0.58g that were recorded in the City of Cushing are typical of an MMI VIII (8) event (PGA > 40%g) as based upon the MMI scale used by USGS, with potential to cause Moderate-to-Heavy damage to structures. These near-source ground accelerations produced by the Cushing Earthquake are significantly higher than the expected median (of approximately 0.1g) from a magnitude 5.0 earthquake [4].

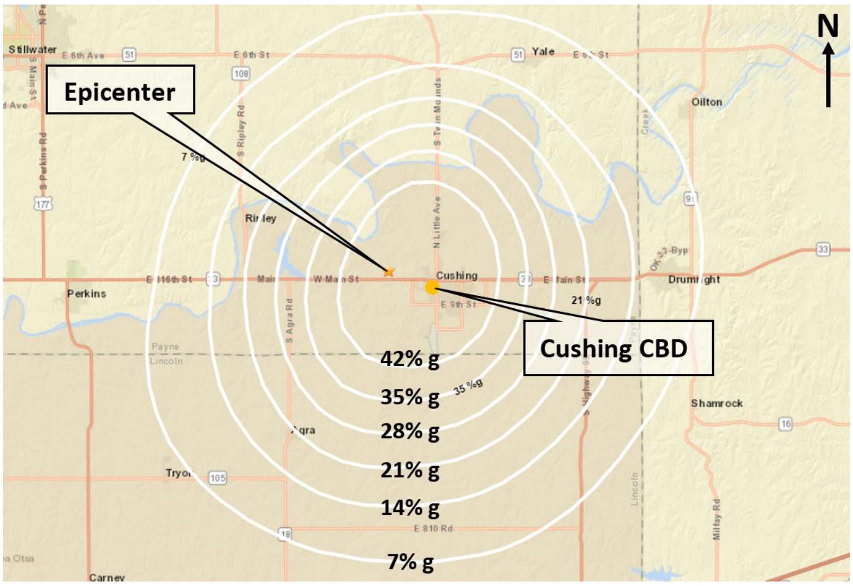

Fig. 1 – Horizontal PGA contour map, USGS [1]

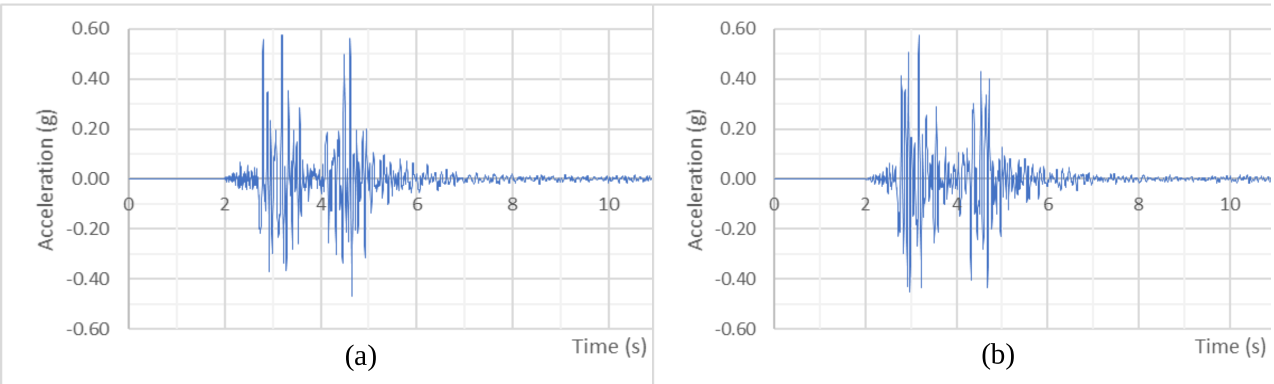

Fig. 2 – Ground acceleration histories [3], seismic station OK914, direction: (a) East-West, (b) North-South

3. Buildings Description

A dozen low-rise buildings were studied which are located 3 to 6 kilometers away from the epicenter of the Cushing Earthquake. These mostly one-story buildings were typically designed and constructed in the last 65 years. Some of the buildings had high ceilings and mezzanine floors.

The structural systems of the buildings under consideration varied. The vertical load carrying systems consist of either steel columns or masonry bearing walls, while the lateral force resisting systems consist of masonry bearing walls. The roof framing consists of either metal deck on steel beams and open-web truss joists or precast concrete roof joists. Concrete slabs on metal deck were also used on the mezzanine floors. Buildings are supported on concrete shallow foundations including grade beams, bell footings, and piers.

The masonry bearing walls that support the roof framing are URM brick walls in the older buildings and concrete masonry unit (CMU) block walls in the later construction. The brick bearing walls are typically 3-wythe thick at the building perimeter and 2-wythe thick at the building interiors. The CMU walls are either unreinforced or lightly reinforced with horizontal steel bars spaced at 1 m. Some of the CMU walls contain vertical steel bars at the jambs of the wall openings. Non-load bearing masonry is also used as interior partition walls and exterior veneers of perimeter cavity walls.

4. Damage Description

Out-of-plumb brick masonry walls were observed including load-bearing walls and exterior veneers of cavity walls (Fig.3). The out-of-plumb masonry was accompanied by horizontal cracks and spalled mortar along the bedjoints of the brick masonry as well as separations of the masonry from the surrounding window frames, stucco, and other wall finishes, which caused cracking and spalling of these finishes.

Out-of-plane damage was also observed in plumb walls in the form of horizontal cracks in the brick masonry and CMU walls, accompanied by spalled mortar, chipped off bricks, and broken blocks along the cracked bedjoint. The cracks were typically located at the base of the walls, the top and the base of wall piers, and emanating from corners of wall openings (Fig.4). Horizontal cracks were also located near mid-height of walls (or higher depending on the connectivity of the top of the wall). The cracks were through-cracks penetrating the thickness of the walls as observed from both sides of the walls and the jambs of the wall openings. The bedjoint cracks extended the length of the walls and wall piers.

Separations were observed at the intersection of the orthogonal masonry walls (Fig.5). The separations continued to the top of the walls above the drop ceilings, accompanied by displaced and deformed grid-framing of the drop ceiling at the wall corners. Where the two intersecting walls were built integral to each other with masonry units that continued past the intersection, the separations continued through the units, resulting in broken and spalled bricks and blocks along the height of the wall intersections. Separations and spalling occurred due to the movement of the walls relative to each other and the out-of-plane action of the orthogonal wall.

In-plane damage to masonry walls was observed coupled with the out-of-plane damage, with stair-stepped cracks through headjoints and bedjoints that continued to the top of the walls above the drop ceilings and stair-stepped cracks that emanated from wall openings (Fig.6). At some locations, cracks penetrated the CMU and broke the concrete block.

Masonry bearing walls exhibited cracking around the bearing locations of the roof joists and beams, as well as split, broken, dislodged, and offset bricks and CMU blocks at these locations (Fig.7, Fig.8, Fig.9). Broken pieces of bricks, CMU blocks, grout, and mortar were observed to have fallen off the top course or the bearing course and laid on top of the suspended ceiling and insulation systems. These observations were indicative of movement and shifting of the roof framing relative to the masonry bearing walls.

In buildings with precast concrete floor and roof framing, cracks, spalls, and offsets in the vicinity of the beam end connections were observed (Fig.10). Spalling of the concrete and CMU wall components also occurred along their interface and connections with steel framing columns and beams (Fig.11).

Damage to wall finishes was widespread and included, among others, cracked drywalls, separations at seams of partition wall panels, and broken ceramic wall tiles (Fig.12). Other non-structural components which sustained damage included architectural components such as ceiling sheathings, suspended ceilings, and roof insulation, as well as mechanical and electrical utilities such as pipework hung from roof framing or ductwork supported by ceiling grid framing (Fig.13).

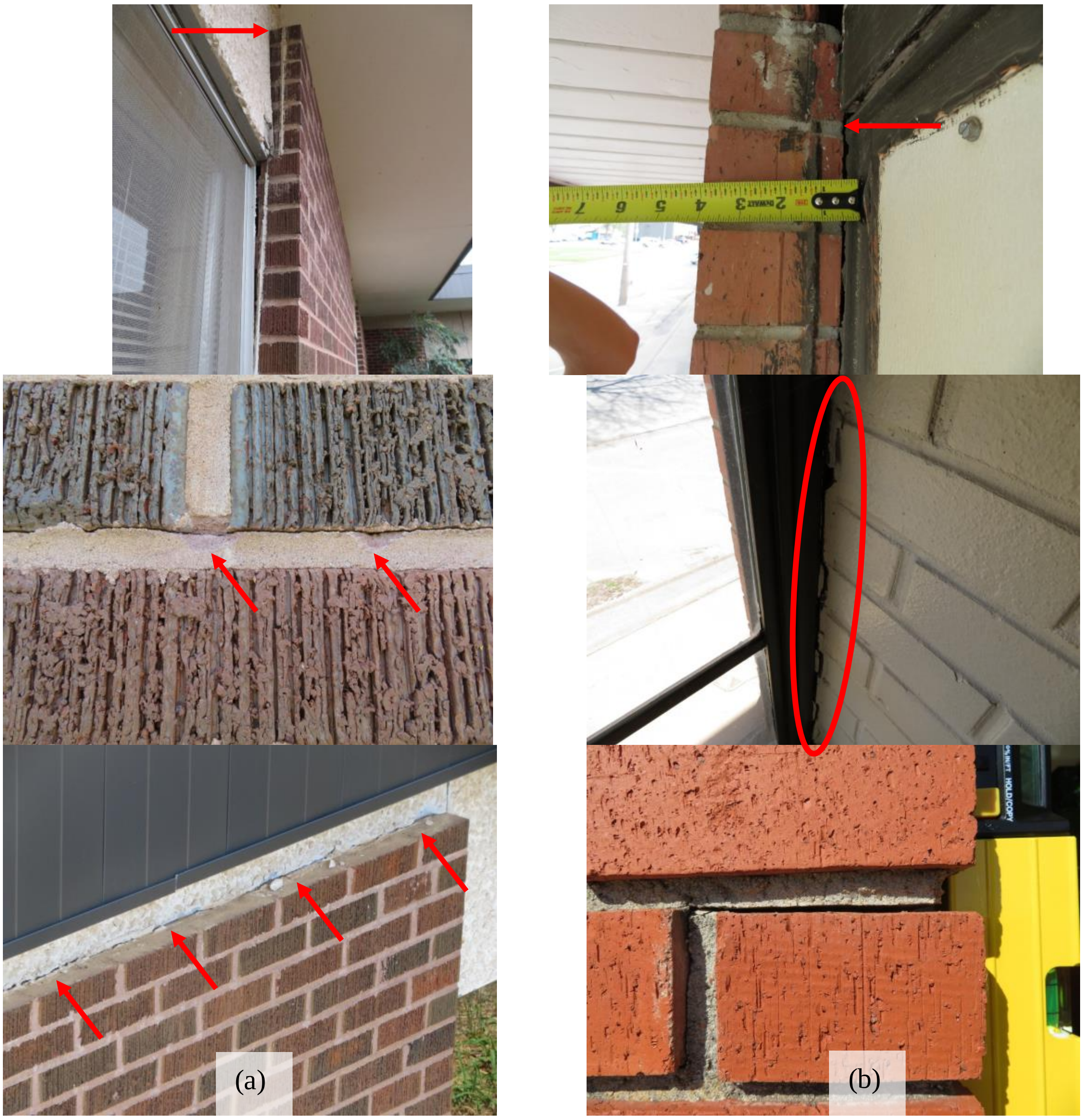

Fig. 3 – Out of-plumb walls: (a) Brick veneers on CMU walls, (b) Load-bearing brick walls

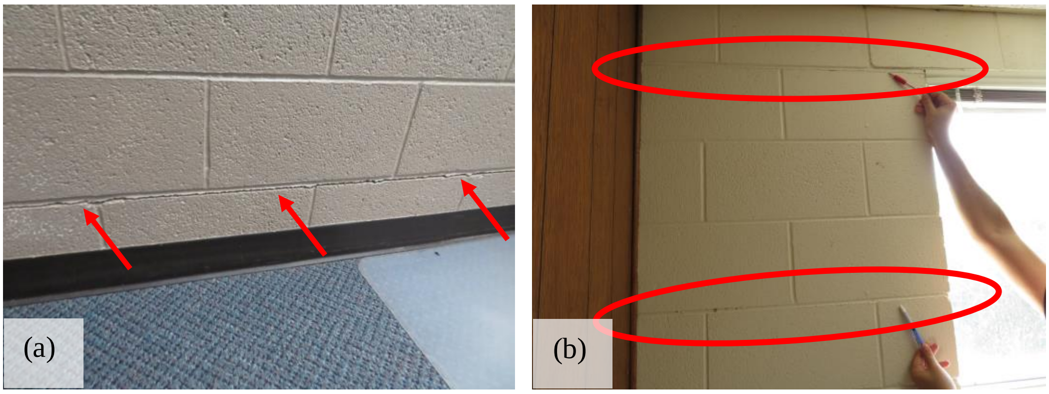

Fig. 4 – Horizontal cracks in CMU bearing walls: (a) At base of wall, (b) At top and mid-height of wall pier

Fig. 5 – Cracks and spalls due to separation between intersecting brick walls

Fig. 6 – Stair-stepped cracks in CMU walls

Fig. 7 – Cracks, spalls, offsets at masonry bearing wall supports of precast concrete roof joists

Fig. 8 – Cracks, spalls, offsets at masonry bearing wall supports of steel roof truss joists

Fig. 9 – Cracks, spalls, offsets at masonry bearing wall supports of steel roof beams

Fig. 10 – Cracks, spalls, offsets at precast concrete beam end connections

Fig. 11 – Cracks and spalls at interface with steel frames

Fig. 12 – Damage to wall finishes

Fig. 13 – Damage to ceilings, roof insulation, utility systems hung from roof framing

5. Structural Analyses

Structural engineering analyses were performed for typical masonry walls at the buildings as part of damage evaluation and repair assessment for the structures.

Force-deformation curves (capacity curves) were developed for representative masonry walls based on the ASCE 41-17 Standard [5]. The strength capacity and the stiffness of each wall were developed based on the concepts of engineering mechanics. The nonlinear post-peak behavior was incorporated using the strength loss parameters described in ASCE 41-17 [5] to develop the capacity curve for each wall idealized as a single-degree-of-freedom (SDOF) mathematical model. The out-of-plane capacity curves for the walls were developed based on Simsir [6] and more recently Khosravikia [7], in conjunction with ASCE 41-17 [5].

Nonlinear dynamic response history analyses of these masonry walls were then performed in the SAP2000 structural analysis computer program [8], incorporating the program's hysteretic models with strength and stiffness deterioration characteristics of inelastic structural response. This represents a numerical simulation of the structures subjected to seismic loading which included computer runs with the ground acceleration histories recorded at the three seismic stations closest to the subject buildings. The cardinal directions of the seismic records were rotated to match the directions of the buildings' orthogonal axes to use the records in the analyses.

Fig.14 shows the in-plane response to ground acceleration history of masonry walls in the direction of the applied seismic load which is parallel to the plane of the walls. These results indicate a significant drop in the lateral strength of the walls, both in the pre-peak and the post-peak ranges of the capacity curves, accompanied with a drop in the lateral stiffness of the walls, as illustrated with dashed lines in Fig.14. The deviation from the capacity curve and associated strength loss is up to 40% for some masonry walls. The inelastic response of the masonry walls during cyclic earthquake loading results in energy dissipation in each cyclic loop (excursion). These loops are evident in Fig.14 and correlate to the damage sustained by these building components such as cracking and spalling of the masonry.

Fig.15 shows the results from the computer analysis runs for a load-bearing and a non-load bearing masonry wall response to ground acceleration history (shown with solid lines). In particular, Fig.15 illustrates the out-of-plane response of two masonry walls in the direction of the applied seismic load which is perpendicular to the plane of each wall. The results of the analyses show that the masonry walls cracked and rocked in the out-of-plane direction during the ground shaking.

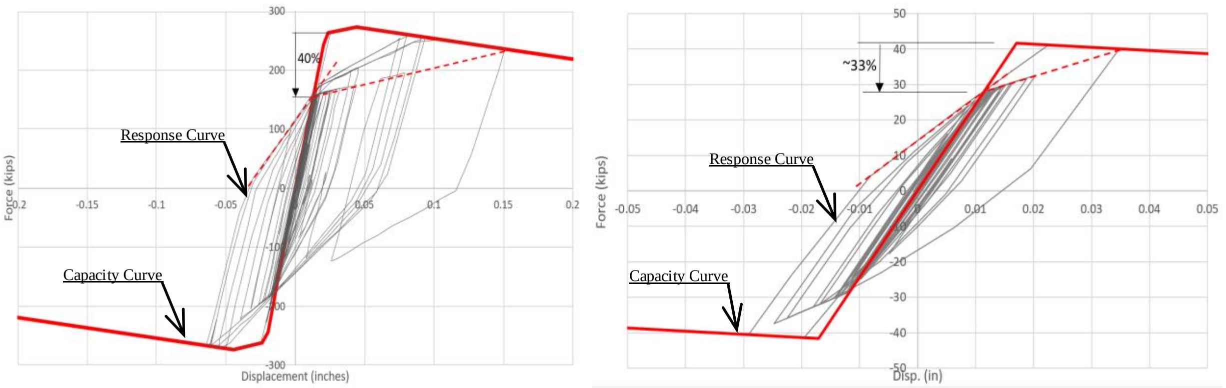

Fig. 14 – In-plane wall response to acceleration history record

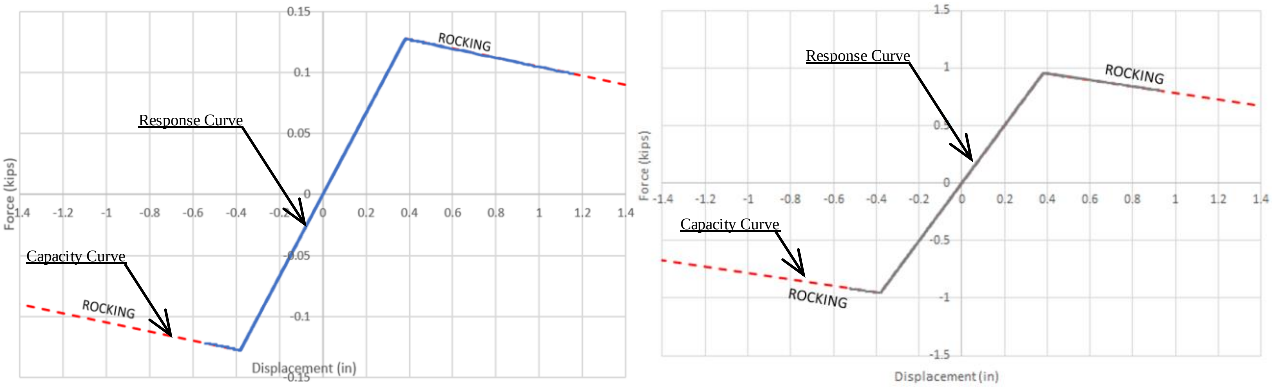

Fig. 15 – Out-of-plane wall response to acceleration history record

7. Damage Analysis and Conclusions

The factors which contributed to the earthquake damage observed at the buildings include the following:

The epicenter of the Cushing Earthquake was in close proximity of the buildings described in this paper and the earthquake focal depth was small, resulting in strong, near-fault ground motions at the building sites.

Due to the combined effects of proximity, shallowness, and directionality, the intensity of shaking during the Cushing Earthquake was much greater than any other in the town's recorded history. The recorded values of ground accelerations in the City of Cushing during the November 6, 2016 earthquake of up to 0.58g were substantial, typically attributed to large magnitude earthquakes. The magnitude of PGA in proximity of the building sites was in the range of 0.42g to 0.58g. These near-source ground accelerations produced by the Cushing Earthquake are significantly higher than the expected median (of approximately 0.1g) from a magnitude 5.0 earthquake [4].

Fig.16 shows the acceleration response spectra as obtained from one of the stations for the Cushing Earthquake. The ground accelerations were amplified by the dynamic characteristics of the low-rise buildings with one-story stiff walls and short periods. The structural engineering analyses described earlier computed a natural period of vibration in the range of approximately 0.04 seconds to 0.12 seconds for the individual masonry walls and the building structures. Spectral accelerations of over 2g in the range of the dominant periods of the earthquake ground motion (between 0.04 and 0.15-seconds) coincided with the natural period of vibration of the masonry walls and the building structures. For instance, a comparison between the spectral acceleration of approximately 1.5g at 0.1-second from Fig.16 and the peak ground acceleration of 0.58g shows that the subject walls experienced about 2.6 times the ground acceleration during the Cushing Earthquake. This striking feature of the Cushing Earthquake with spectral amplification near the 0.1-second period was also illustrated in literature [4].

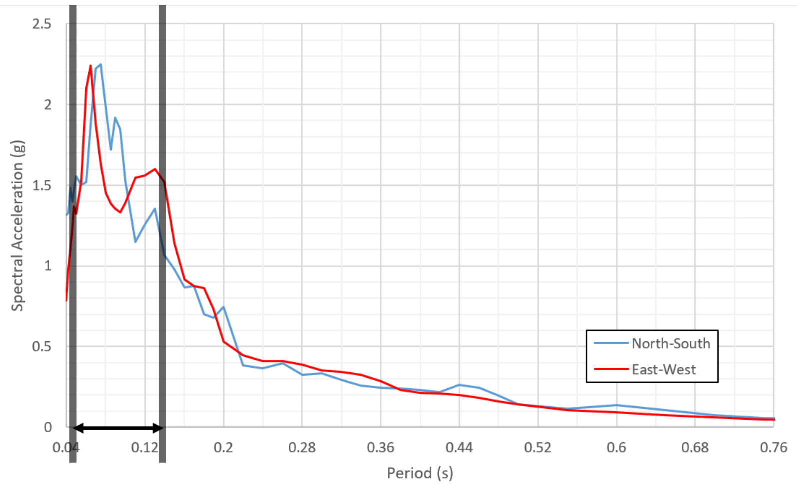

Fig. 16 – Acceleration response spectra (5% damped) at seismic recording station OK914

The buildings evaluated for this study were designed and constructed with little consideration for seismic actions. This is because they are located in an intraplate region with limited seismic history; therefore, the building codes [9] that were in effect at the time of their design and construction (1955-1990) assigned small design earthquake loads compared to regions of moderate or high seismicity. This design earthquake load was smaller than the design wind load which governed the building design and therefore no seismic detailing of building components was provided. Therefore, the design response spectrum for the building was an order of magnitude smaller than the response spectra recorded during the Cushing Earthquake.

The flexible diaphragms of the steel framed roofs of the buildings resulted in increased seismic displacements of the roof framing and amplified deformation demands on the non-structural components such as the roof insulation, ceilings, and utility lines that are connected to the roof framing. It also resulted in increased seismic displacements of the walls that are orthogonal to the ground motion direction. This amplified the earthquake deformation demand and out-of-plane cracking and rocking in the masonry walls.

Ceiling damage occurred more severely along the masonry walls than elsewhere based on on-site observations. This was an indication of out-of-plane movement of masonry walls against the ceilings, causing deformation, cracking, buckling, and collapse of ceilings. Ceiling damage was one of the indicators of out-of-plane movement and rocking of masonry walls, as well as an indicator of in-plane deformation of roof diaphragms.

Damage due to out-of-plane wall movement included horizontal cracks across the masonry walls, out-of-plumb walls, and separations from the orthogonal walls as observed. Out-of-plane wall damage was observed to load bearing masonry walls as well as non-load bearing masonry walls and veneers. The structural analysis results also indicated that the walls cracked and rocked in the out-of-plane direction due to the Cushing Earthquake, thus corroborating the damage observations.

In addition, in-plane wall damage in the form of stair-stepped cracking of the masonry walls was also corroborated with structural analysis results.

In contrast to the steel framed roofs, the precast concrete rigid diaphragms resulted in increased seismic mass and inertia. This amplified the earthquake force demand and cracking in the masonry walls.

At locations of roof joists bearing on masonry walls, observations revealed cracking and spalling of the masonry walls and spalling of the precast concrete beams in the vicinity of their end connections.

The loss in strength and stiffness of the damaged lateral force resisting components, such as the masonry walls, makes them weaker and softer so that they would sustain much greater damage if they were subjected to an event similar to the Cushing Earthquake again due to their reduced ability to dissipate earthquake energy. Repairs to the damaged building components should target the recovery of any strength and stiffness that were lost during the earthquake in order to restore the buildings to their pre-earthquake condition and also to prevent long-term maintenance issues such as cracks re-appearing through the wall finishes over time or during future seismic events.

Repairs should also include strengthening of the lateral force resisting system with substantial structural damage in compliance with IEBC 2015 [10]. This includes some of the CMU walls as shown in our analysis. The strengthening design needs to meet either the 75% of the IBC 2015-level [11] seismic forces for the Risk Category of the buildings or the Damage Control Structural Performance per ASCE 41-17 [5].

In the last 10 years, rates of earthquakes increased rapidly in Oklahoma; consequently, the USGS updated the short-term seismic hazard maps for the region in the last three years to account for induced earthquakes [1]. Therefore, the authors recommend that the strengthening design also consider this updated induced earthquake hazard in addition to the IBC 2015 [11] natural earthquake hazard. The strengthening design spectral acceleration may be taken as 75% of two-thirds of the curve B in Fig.17 [1, 4]. This corresponds to approximately 1.4g at the fundamental period of the buildings (or roughly a repeat of the Cushing Earthquake for existing buildings when compared to Fig.16 at the 0.1-second period).

The strengthening work for the lateral force system with substantial damage would typically include, along with the repairs, strengthening of the connections between the masonry walls and the roof framing to provide improved load path continuity to support and transfer seismic load demands for roof diaphragm action. Strengthening for the induced earthquake hazard would include, in addition to the above, installation of reinforced concrete overlay or carbon fiber reinforced polymer (CFRP) fabric sheets on some of the masonry walls.

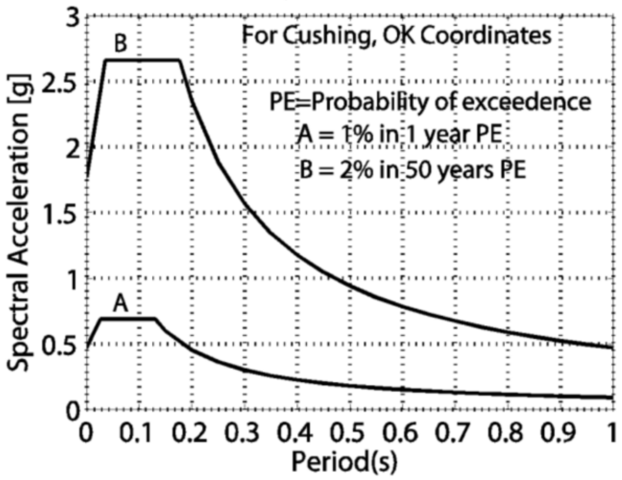

Fig. 17 – Induced earthquake hazard response spectra for Cushing, USGS [1, 4]

8. Acknowledgements

The authors wish to thank Dr. Mohammad Moravej and Ms. Maanasa Vemuri for their contributions to the collection of on-site data, and Mr. Daren Reyes for assisting in the processing of this data.

9. References

[1] USGS (2019), https://earthquake.usgs.gov/ *United States Geological Survey*. USA.

[2] Delatte N, Greer A (2018): Earthquakes in Oklahoma – Adapting to a new reality. *Proceedings of the Forensic Engineering 8th Congress, American Society of Civil Engineers*. Austin, TX, USA.

[3] CESMD (2019), https://www.strongmotioncenter.org/ *Center for Engineering Strong Motion Data*. USA.

[4] EERI (2017): Earthquake Reconnaissance Team Report: M5.0 Cushing, Oklahoma, USA Earthquake on November 7, 2016. *Earthquake Engineering Research Institute*. USA.

[5] ASCE (2017): ASCE Standard, ASCE/SEI 41-17, Seismic Evaluation and Retrofit of Existing Buildings. *American Society of Civil Engineers*. Reston, VA, USA.

[6] Simsir CC (2004): Influence of Diaphragm Flexibility on the Out-of-Plane Dynamic Response of Unreinforced Masonry Walls. *Ph.D. Dissertation*. University of Illinois at Urbana-Champaign, Urbana, IL, USA.

[7] Khosravikia F, Kurkowski J, Clayton P (2020): Fragility of masonry veneers to human-induced Central U.S. earthquakes using neural network models. *Journal of Building Engineering*, **28**.

[8] CSI (2019): SAP2000 v21.0.2, Structural Analysis Program, *Computers and Structures, Inc*. USA.

[9] BOCA: BOCA Basic Building Code. *Building Officials and Code Administrators International*. USA.

[10] IEBC (2015): International Existing Building Code. *International Code Council, Inc*. USA.

[11] IBC (2015): International Building Code. *International Code Council, Inc*. USA.

